Universal Relations Among Neuron Star Parameters

Martin Urbanec
Silesian University in Opava, Czech Republic

Brainstorming Workshop
Deciphering neutron star equation of state
Warsaw, August 5 2024

Motivation

- Neutron star mergers are large colliders provided for free by Universe
  - Price we pay is limited knowledge of what is collided
- Study of colliding neutron stars can help us to
  - Constrain physics of dense matter
  - Study cosmology
  - Understand astrophysics (kilonova, GRBs)
  - Study “chemical” evolution of the universe (NS mergers are main events where some elements are created – Au, Pt …)

Equation of state

- From nuclear physics: Binding energy as a function of baryon density and composition
- NS equilibrium – charge neutrality + equilibrium (e.g. β) -> e(n)
- First law of thermodynamics -> $P=n^2\,\partial e/\partial n$
- Equation of state in the form P(e)

- Different ways how to describe nucleon-nucleon interaction
  - Both theoretical – (semi)analytical, from effective Hamiltonian etc.
  - Each theoretical description has parameters that can differ from one EoS to another – parameterizations

Equation of state -> NS model (nonrotating)

- Spherical symmetric space-time $\mathrm{d}s^2 = -\mathrm{e}^{2\nu}\,\mathrm{d}t^2 + \mathrm{e}^{2\lambda}\,\mathrm{d}r^2 + r^2(\mathrm{d}\theta^2 + \sin^2\theta\,\mathrm{d}\phi^2),$

- Perfect fluid $T^{\mu\nu} = (\mathscr{E} + P)U^\mu U^\nu + P g^{\mu\nu},$

- From Einstein equations:

$$\frac{\mathrm{d}\nu}{\mathrm{d}r} = -\frac{1}{\mathscr{E}+P}\frac{\mathrm{d}P}{\mathrm{d}r},$$

$$\mathrm{e}^{2\lambda} = \left(1 - \frac{2m(r)}{r}\right)^{-1}.$$

- From conservation of energy momentum tensor: $\dfrac{\mathrm{d}P}{\mathrm{d}r} = -(\mathscr{E}+P)\dfrac{m(r) + 4\pi r^3 P}{r(r-2m(r))},$

Equation of state -> NS model

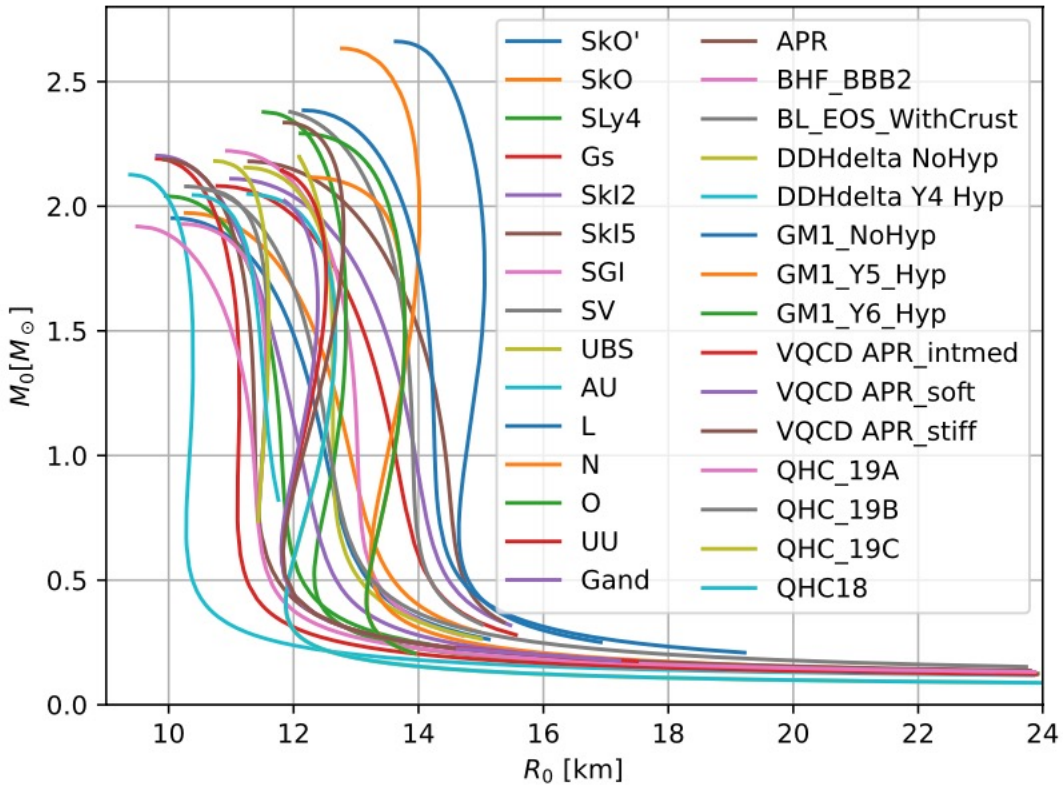

Equations of state taken from the compose database

(https://compose.obspm.fr)

[TOK_2015] S. Typel, M. Oertel, T. Klähn, Phys.Part.Nucl. 46, 633

[OHKT_2017] M. Oertel, M. Hempel, T. Klähn, S. Typel, Rev. Mod. Phys. 89, 015007

[TOK_2022] S. Typel, M. Oertel, T. Klähn et al, arxiv:2203.03209

There are dozens of models with hundreds of parametrizations

Universal relations – first results

- Ravenhall & Pethick 1994 –Neutron star moments of inertia

$$ds^2 = -e^{\nu(r)}\,dt^2 + e^{\lambda(r)}\,dr^2 + r^2(d\theta^2 + \sin^2\theta\,d\phi^2)\,.$$

$$\frac{dP}{dr} = -\frac{(\rho + P/c^2)G(m + 4\pi r^3 P/c^2)\Lambda(r)}{r^2}\,, \qquad \frac{dm}{dr} = 4\pi r^2 \rho\,,$$

$$\Lambda(r) = e^{\lambda(r)} = [1 - 2Gm(r)/rc^2]^{-1}$$

$$\frac{d}{dr}\left(r^4 j \frac{d\varpi}{dr}\right) = -4r^3 \frac{dj}{dr}\,\varpi\,.$$

$$I = -\frac{2c^2}{3G}\int_0^R r^3 \frac{dj(r)}{dr}\frac{\varpi(r)}{\Omega}\,dr$$

$$= \frac{8\pi}{3}\int_0^R r^4\left(\rho + \frac{P}{c^2}\right)\Lambda(r) j(r)\,\frac{\varpi(r)}{\Omega}\,\mathrm{dr}$$

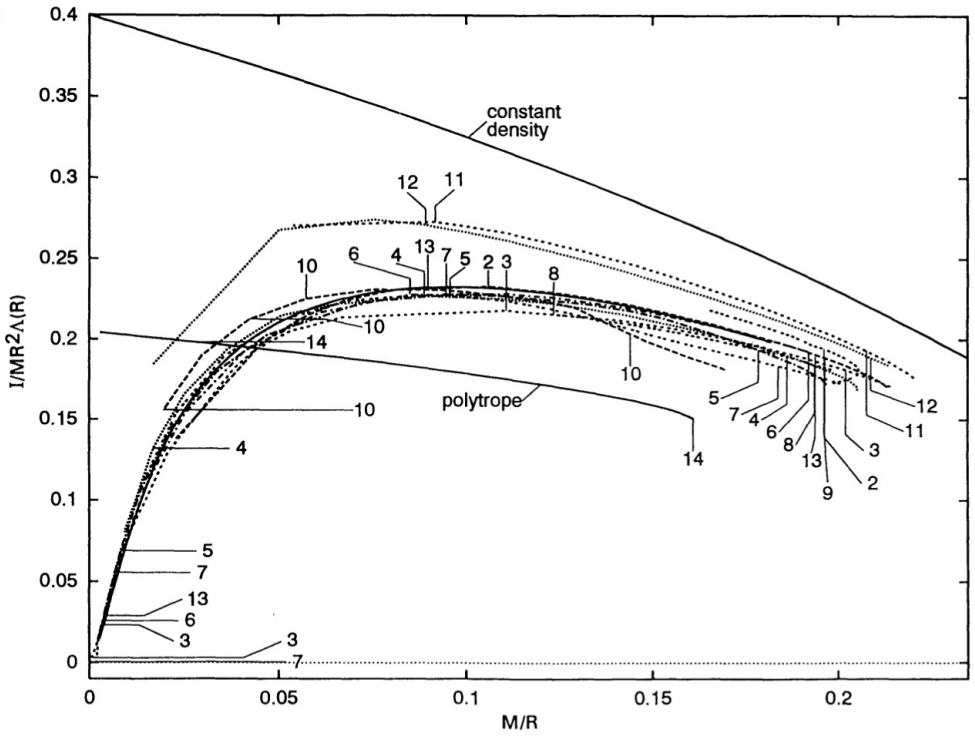

FIG. 4.—The quantity $I/MR^2\Lambda(R)$ as a function of M/R (M in $M_\odot$, R in km), for the values contained in the Tables of Arnett & Bowers (1977). Indicated on each curve is the point closest to the maximum mass (downward vertical line) and to $M = 1\,M_\odot$ (upward vertical line); also, where available, the point at which the central baryon density is close to $n_s = 0.16\ \mathrm{fm}^{-3}$, and that where it is close to the density of the liquid-solid phase transition (short and long horizontal lines, respectively). The number attached to the points refers to the Tables in Arnett and Bowers cited in our Table 1. Curves are also included for the FPS equation of state (see footnote 1), numbered 13, the general-relativistic incompressible-fluid model (Chandrasekhar & Miller 1974), and the polytrope $\nu = 5/3$, respresenting a gas of free neutrons, numbered 14.

Universal relations – first results

- Bejger & Haensel 2002 “Moments of inertia for neutron and strange stars: Limits derived for Crab pulsar”

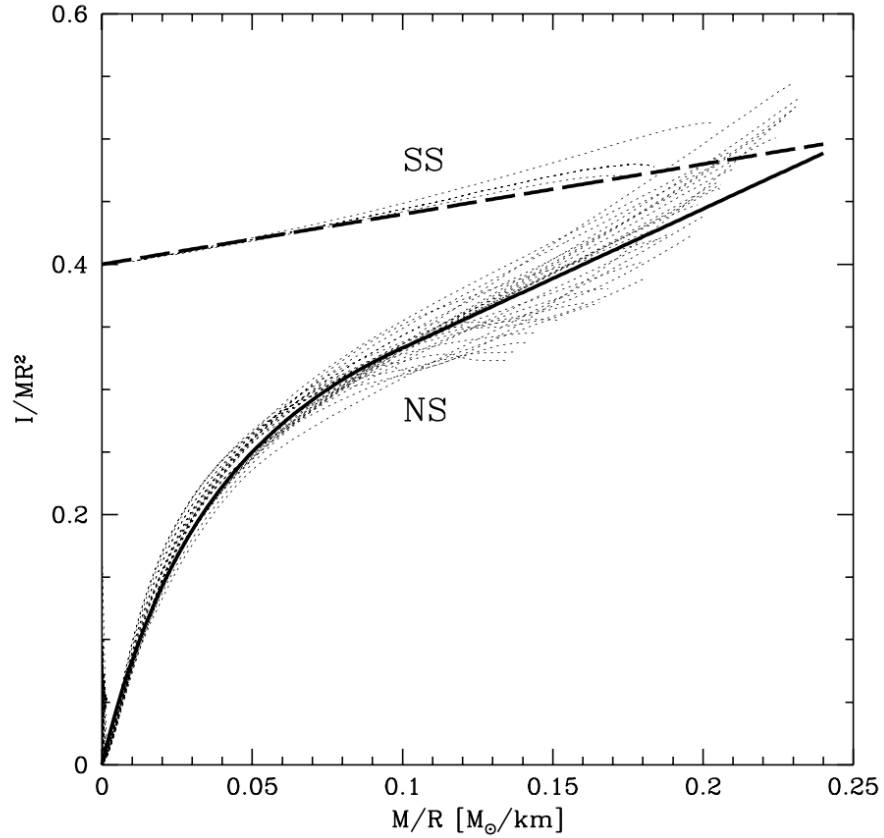

Fig. 1. The ratio I/MR^2 versus compactness parameter M/R for selected set of EOSs of dense matter. Branches NS and SS correspond to neutron stars and strange stars. Thick lines were obtained using the analytical fitting formulae (solid – NS, dashed – SS), described in the text. Both thick lines are terminated at the M/R upper-bound for the EOS respecting condition $v_{\rm sound} \leq c$, which is equal 0.24.

Universal relations 2013 and beyond

- Three groups published discussing universal relations
- Urbanec, Miller, Stuchlík: Quadrupole moments of rotating neutron stars and strange stars, (MNRAS)
- Yagi & Younes: I-Love-Q: Unexpected Universal Relations for Neutron Stars and Quark Stars (Science), I-Love-Q relations in neutron stars and their applications to astrophysics, gravitational waves, and fundamental physics (PRD)
- Maselli, Cardoso, Ferrari, Gualtieri, Pani: Equation-of-state-independent relations in neutron stars (PRD)

- Later studied for magnetic stars, in alternative gravities, for hot stars etc.

Rotating stars – C-Q relations

- Hartle Thorne approach (slow rotation)

$$
\begin{aligned}
\mathrm{d}s^2 = & -\mathrm{e}^{2\nu}[1+2h_0(r)+2h_2(r)P_2]\mathrm{d}t^2 \\
& +\mathrm{e}^{2\lambda}\left\{1+\frac{\mathrm{e}^{2\lambda}}{r}[2m_0(r)+2m_2(r)P_2]\right\}\mathrm{d}r^2 \\
& +r^2[1+2k_2(r)P_2]\left\{\mathrm{d}\theta^2+[\mathrm{d}\phi-\omega(r)\mathrm{d}t]^2\sin^2\theta\right\},
\end{aligned}
$$

- Differential equations for perturbation functions are obtained from Einstein equations
- We match exterior and interior solution

-> *M, J, Q*

Rotating stars – C-Q relations

- Hartle Thorne approach (slow rotation)

$$
\begin{aligned}
\mathrm{d}s^2 = & -\mathrm{e}^{2\nu}[1+2h_0(r)+2h_2(r)P_2]\mathrm{d}t^2 \\
& +\mathrm{e}^{2\lambda}\left\{1+\frac{\mathrm{e}^{2\lambda}}{r}[2m_0(r)+2m_2(r)P_2]\right\}\mathrm{d}r^2 \\
& +r^2[1+2k_2(r)P_2]\left\{\mathrm{d}\theta^2+[\mathrm{d}\phi-\omega(r)\mathrm{d}t]^2\sin^2\theta\right\},
\end{aligned}
$$

- Differential equations for perturbation functions are obtained from Einstein equations
- We match exterior and interior solution

-> *M, J, Q*

Rotating stars – C-Q relations

- Eq. for angular momentum of matter with respect to dragging of in. frames

$$\frac{1}{r^3}\frac{\mathrm{d}}{\mathrm{d}r}\left(r^4 j(r)\frac{\mathrm{d}\tilde{\omega}}{\mathrm{d}r}\right)+4\frac{\mathrm{d}j}{\mathrm{d}r}\tilde{\omega}=0, \qquad \tilde{\omega}(r)=\Omega-\omega(r).$$

- Surface: $\tilde{\omega}(r)=\Omega-\frac{2J}{r^3}, \quad J=\frac{R^4}{6}\left(\frac{\mathrm{d}\tilde{\omega}}{\mathrm{d}r}\right)_{r=R}$

$$\begin{aligned}
\frac{\mathrm{d}m_0}{\mathrm{d}r} &= 4\pi r^2(\mathscr{E}+P)\frac{\mathrm{d}\mathscr{E}}{\mathrm{d}P}p_0+\frac{1}{12}r^4 j^2\left(\frac{\mathrm{d}\tilde{\omega}}{\mathrm{d}r}\right)^2-\frac{1}{3}r^3\tilde{\omega}^2\frac{\mathrm{d}j^2}{\mathrm{d}r},\\
\frac{\mathrm{d}p_0}{\mathrm{d}r} &= -\frac{m_0(1+8\pi r^2 P)}{(r-2m)^2}-\frac{4\pi(\mathscr{E}+P)r^2}{r-2m}p_0+\frac{1}{12}\frac{r^4 j^2}{r-2m}\left(\frac{\mathrm{d}\tilde{\omega}}{\mathrm{d}r}\right)^2\\
&\quad+\frac{1}{3}\frac{\mathrm{d}}{\mathrm{d}r}\left(\frac{r^3 j^2\tilde{\omega}^2}{r-2m}\right),
\end{aligned}$$

$$\begin{aligned}
\frac{\mathrm{d}v_2}{\mathrm{d}r} &= -2\frac{\mathrm{d}v_0}{\mathrm{d}r}h_2+\left(\frac{1}{r}+\frac{\mathrm{d}v_0}{\mathrm{d}r}\right)\left[\frac{1}{6}r^4 j^2\left(\frac{\mathrm{d}\tilde{\omega}}{\mathrm{d}r}\right)^2-\frac{1}{3}r^3\tilde{\omega}^2\frac{\mathrm{d}j^2}{\mathrm{d}r}\right],\\
\frac{\mathrm{d}h_2}{\mathrm{d}r} &= -\frac{2v_2}{r(r-2m(r))\mathrm{d}v_0/\mathrm{d}r}\\
&\quad+\left\{-2\frac{\mathrm{d}v_0}{\mathrm{d}r}+\frac{r}{2(r-2m(r))\mathrm{d}v_0/\mathrm{d}r}\left[8\pi(\mathscr{E}+P)-\frac{4m(r)}{r}\right]\right\}h_2\\
&\quad+\frac{1}{6}\left[r\frac{\mathrm{d}v_0}{\mathrm{d}r}-\frac{1}{2(r-2m(r))\mathrm{d}v_0/\mathrm{d}r}\right]r^3 j^2\left(\frac{\mathrm{d}\tilde{\omega}}{\mathrm{d}r}\right)^2\\
&\quad-\frac{1}{3}\left[r\frac{\mathrm{d}v_0}{\mathrm{d}r}+\frac{1}{2(r-2m(r))\mathrm{d}v_0/\mathrm{d}r}\right]r^2\tilde{\omega}^2\frac{\mathrm{d}j^2}{\mathrm{d}r}.
\end{aligned}$$

Dimensionless, frequency ind. quantities

- Nonrotating star M_0 R_0
- Rotating stars M, Q, J, f, R_{eq}, R_p
- Dimensionless, frequency independent quantities

  R_0/M_0, QM_0/J^2, I/M^3 $(I=J/f)$

- In the past different normalization of I used (I/MR^2)

Urbanec, Miller, Stuchlík 2013

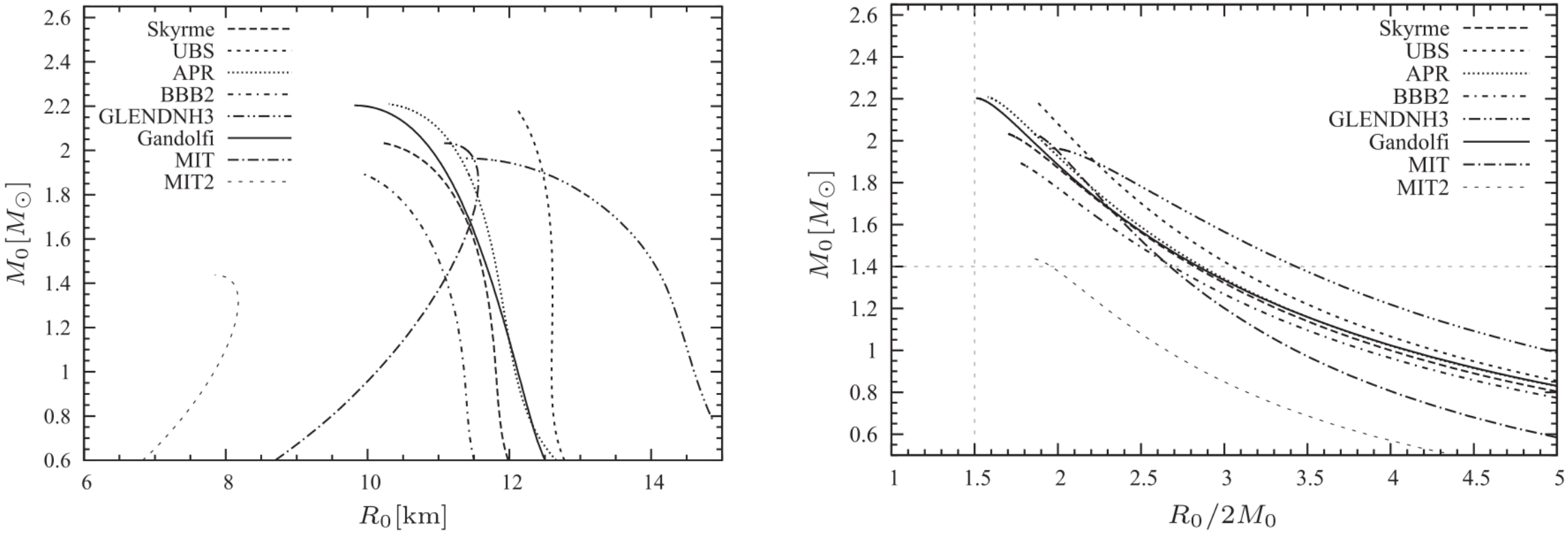

Figure 1. Mass versus radius (left) and $x = R_0/2M_0$ (right) for non-rotating models with the selected equations of state.

Urbanec, Miller, Stuchlík 2013

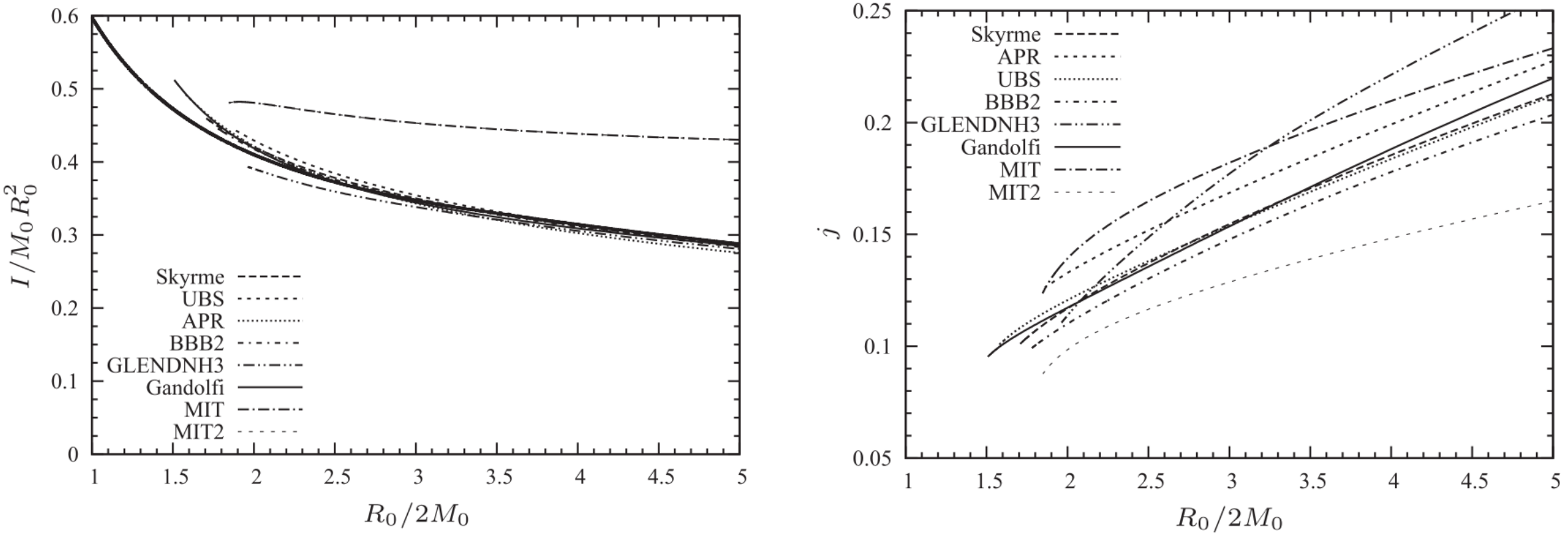

Figure 2. Left: the moment of inertia factor $I/M_0R_0^2$ plotted versus $x = R_0/2M_0$ for the selected equations of state. The curve given by the 'universal' formula is shown with the heavy solid line. Right: the angular momentum parameter $j = J/M_0^2$ for objects rotating at 300 Hz plotted versus $x = R_0/2M_0$.

Urbanec, Miller, Stuchlík 2013

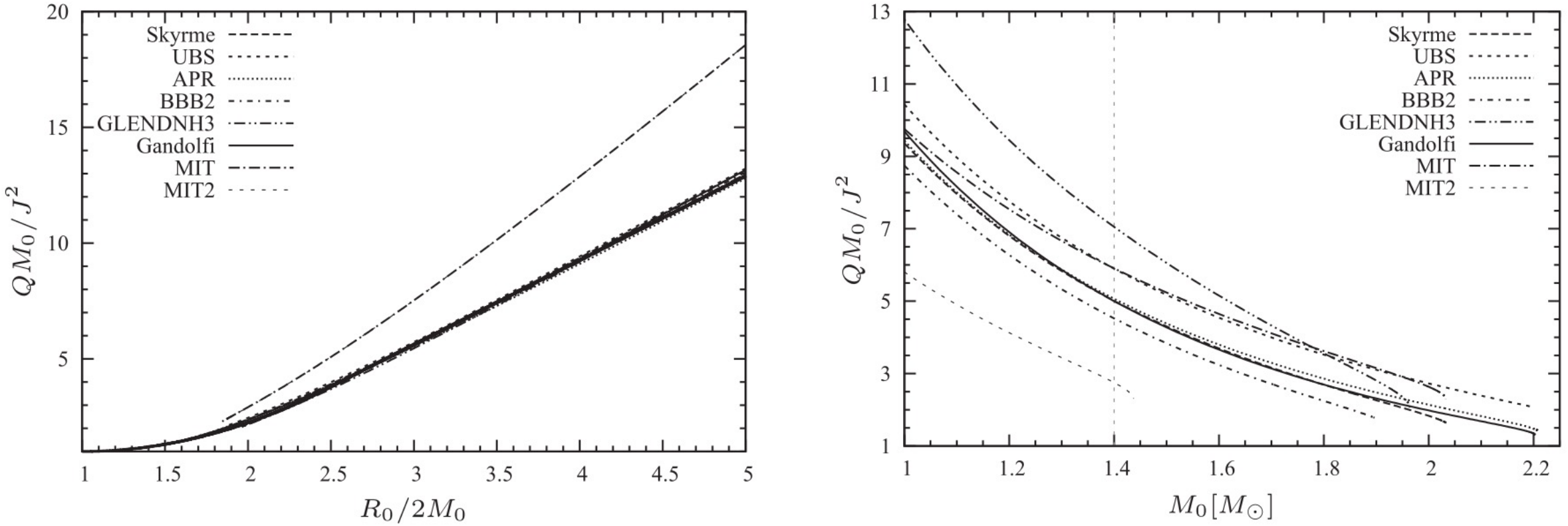

Figure 3. The Kerr factor $\tilde{q} = QM_0/J^2$ as calculated with the selected equations of state. In the left-hand frame, it is plotted against $x = R_0/2M_0$, with the approximate analytic relation (labelled as 'fit') being shown using the heavy solid line. In the right-hand frame, it is plotted against the stellar mass.

Tidal deformability and Love numbers

- Q_ℓ … quadrupolar deformation of gr. field induced by exterior tidal field E_ℓ
- $Q_{\ell m} = -\lambda E_{\ell m}$
- Tidal deformability λ
- Normalized tidal deformability λ/M^5

Yagi & Yunes 2013 PRD

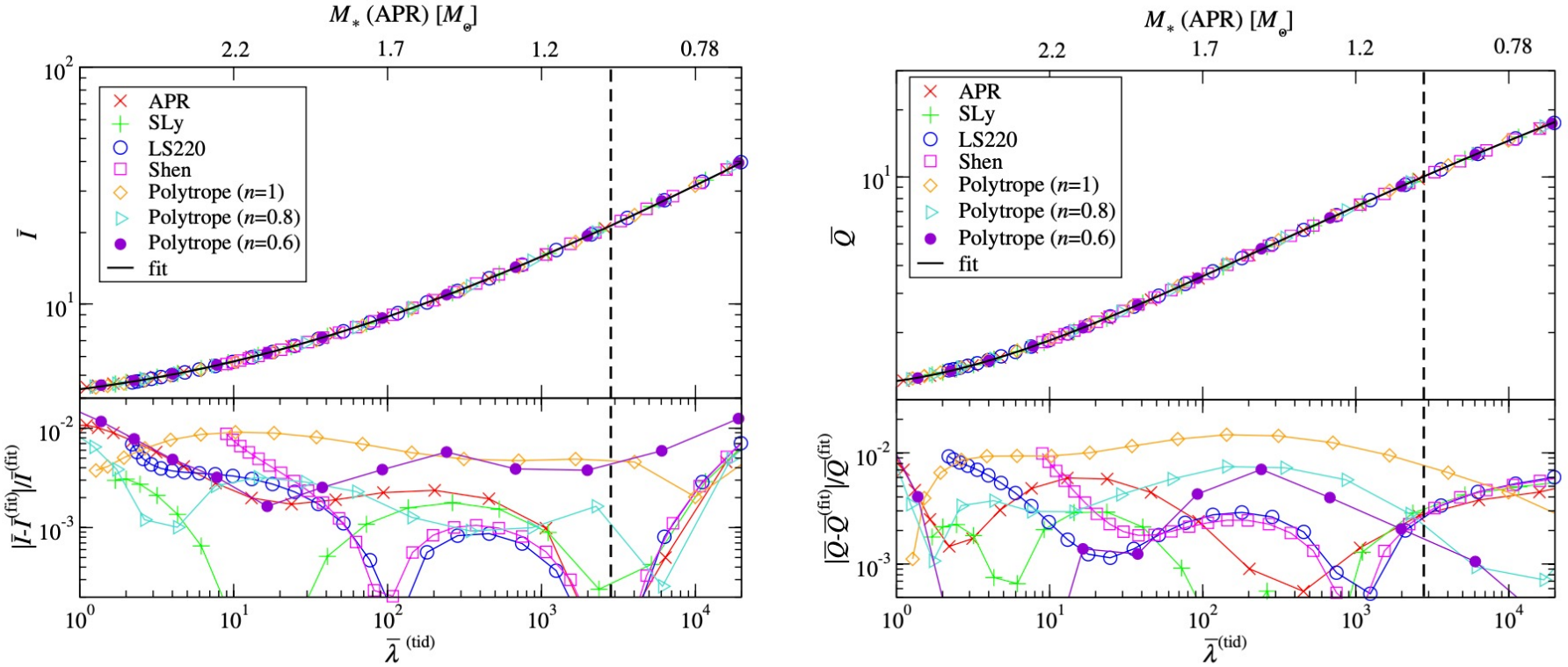

FIG. 1 (color online). (Top) Fitting curves (solid curve), given in Eq. (54), and numerical results (points) of the universal I-Love (left) and Q-Love (right) relations for various EoSs. These quantities are normalized as follows: $\bar{I} = I/M_*^3$, $\bar{\lambda}^{(\rm tid)} = \lambda^{(\rm tid)}/M_*^5$ and $\bar{Q} = Q^{(\rm rot)}/[M_*^3(S/M_*^2)^2]$. The parameter varied along each curve is the NS central density, or equivalently the NS compactness, with the latter increasing to the left of the plots. For reference, we also show the corresponding NS mass for the APR EoS on the top axes and a vertical dashed line when $M_* = 1M_\odot$. (Bottom) Relative fractional errors between the fitting curve and numerical results. Observe that these relations are essentially EoS independent, with loss of universality at the 1% level.

Yagi & Yunes 2013 -Science

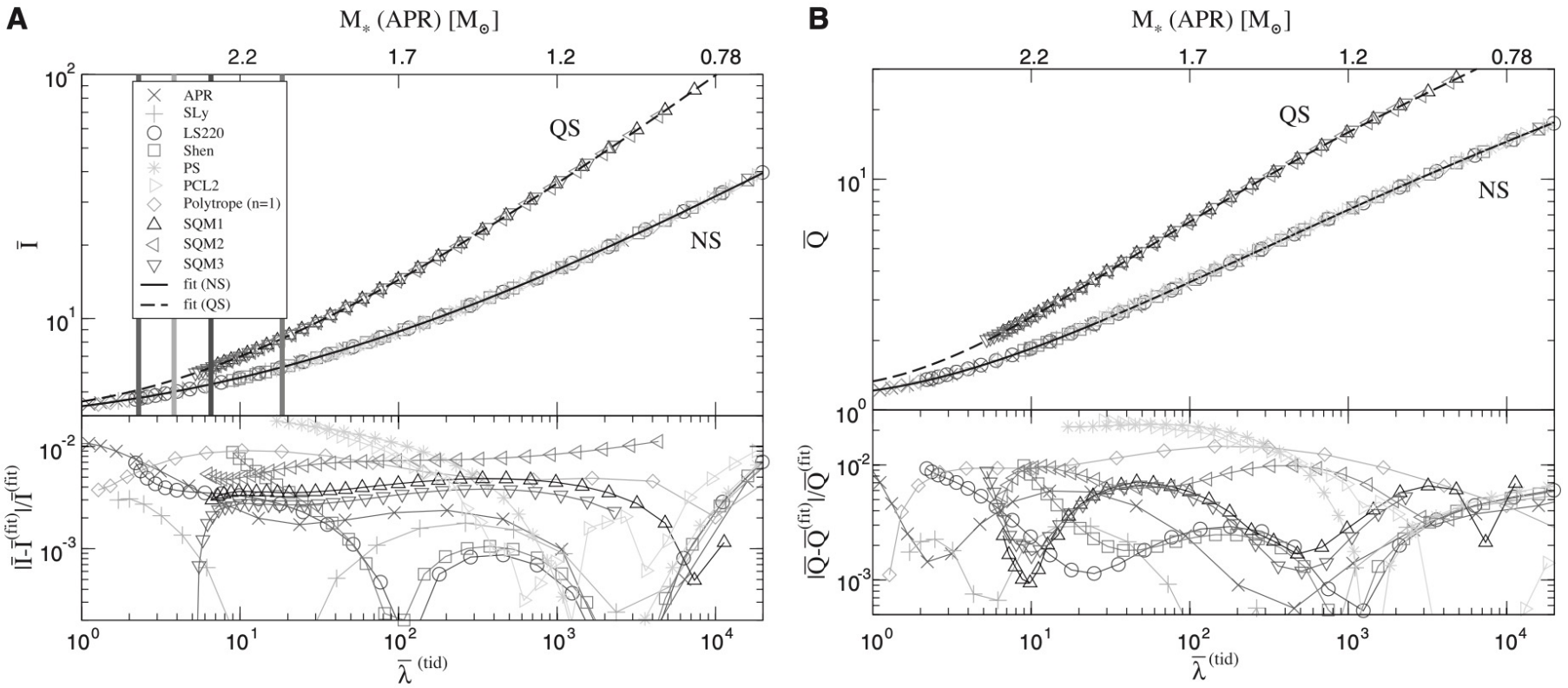

Fig. 1. I-Love and Q-Love relations. (A and **B)** (Top) The neutron star (NS) and quark star (QS) universal I-Love and Love-Q relations for various EoSs, together with fitting curves (solid and dashed curves). On the top axis, we show the corresponding NS mass with an APR EoS. The thick vertical lines show the stability boundary for the APS, SLy, LS220, and Shen EoSs from left to right. The parameter varied along each curve is the NS central density, or equivalently the NS compactness, with the latter increasing to the left of the plots. (Bottom) Fractional errors between the fitting curves and numerical results. $M_\odot$ indicates the mass of the Sun.

Love numbers and tidal deformability

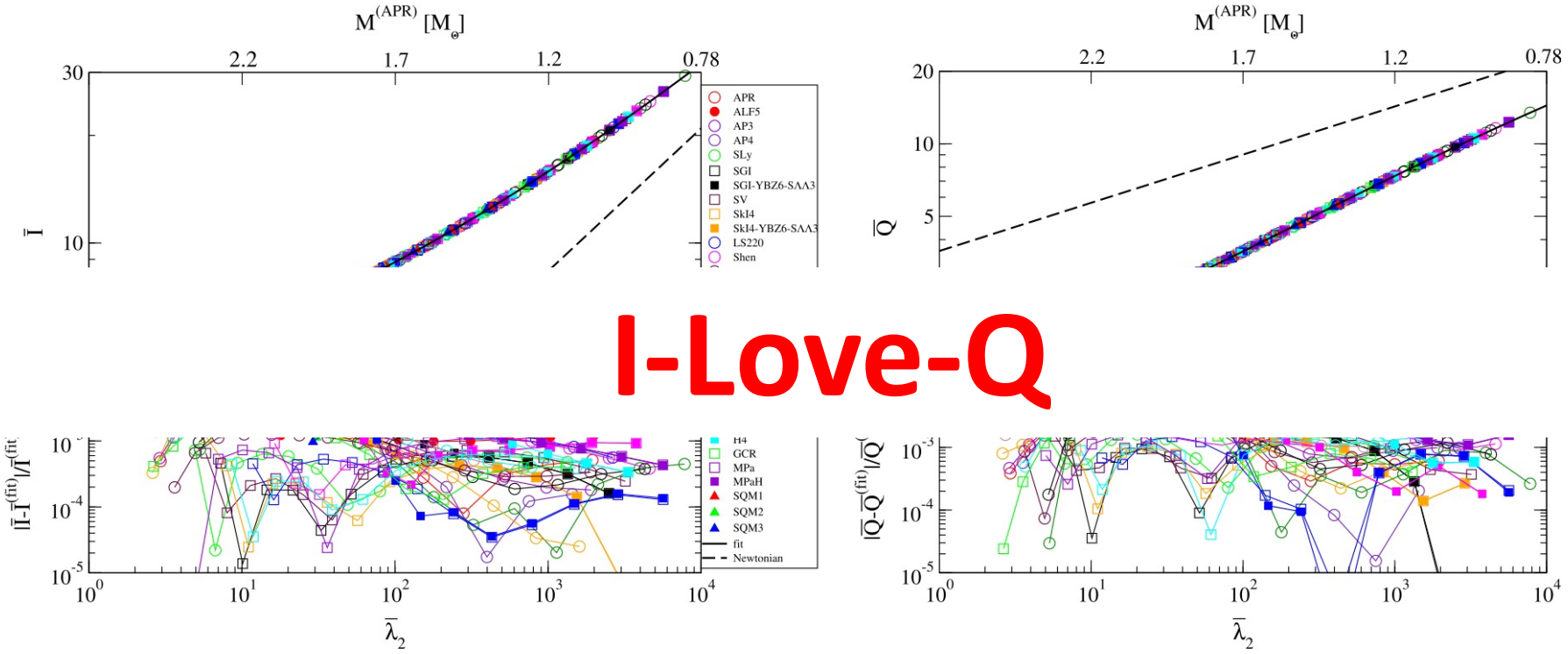

I-Love-Q

Fig. 3. (Top) The universal I–Love (left) and Q–Love (right) relations for slowly-rotating neutron stars and quark stars of $1M_\odot < M < M^{(\max)}$ with various equations of state. A single parameter along the curve is the stellar mass or compactness, which increases to the left of the plots. The solid curves show the fit in Eq. (15). The top axis shows the corresponding stellar mass of an isolated, non-rotating configuration with the APR equation of state. (Bottom) Absolute fractional difference from the fit, while the dashed lines show the analytic Newtonian relations in Eq. (11) with $n = 0$. Observe that the relations are equation-of-state insensitive to $\mathcal{O}(1\%)$.

Yagi & Yunes, 2017, Phys. Rep.

New calculations

- EoS from CompOSE
- Rotating stars M, Q, J, f, R_{eq}, R_p
- Dimensionless, frequency independent quantities
  - R_0/M_0, QM_0/J^2, I/M^3

- New quantities related to the change of the shape of the star and the increase in gravitational mass

$$M = M_0 + \delta M = M_0 + m_0(R) + J^2/R^3$$

$$\begin{aligned} R_{\rm eq} &= R + \xi_0(R) - \frac{1}{2}\xi_2(R), \\ R_{\rm p} &= R + \xi_0(R) + \xi_2(R). \end{aligned}$$

Equation of state -> NS model

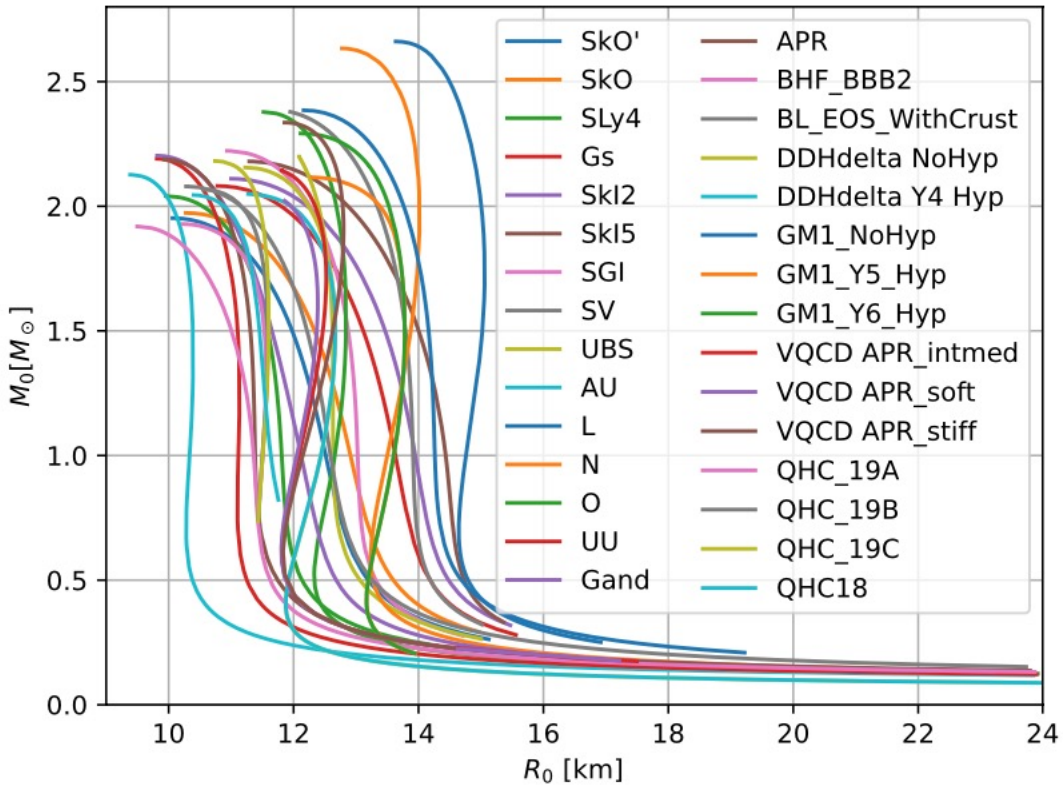

Equations of state taken from the compose database

(https://compose.obspm.fr)

[TOK_2015] S. Typel, M. Oertel, T. Klähn, Phys.Part.Nucl. 46, 633

[OHKT_2017] M. Oertel, M. Hempel, T. Klähn, S. Typel, Rev. Mod. Phys. 89, 015007

[TOK_2022] S. Typel, M. Oertel, T. Klähn et al, arxiv:2203.03209

There are dozens of models with hundreds of parametrizations

Rotating stars

- Moment of inertia and quadrupole moment

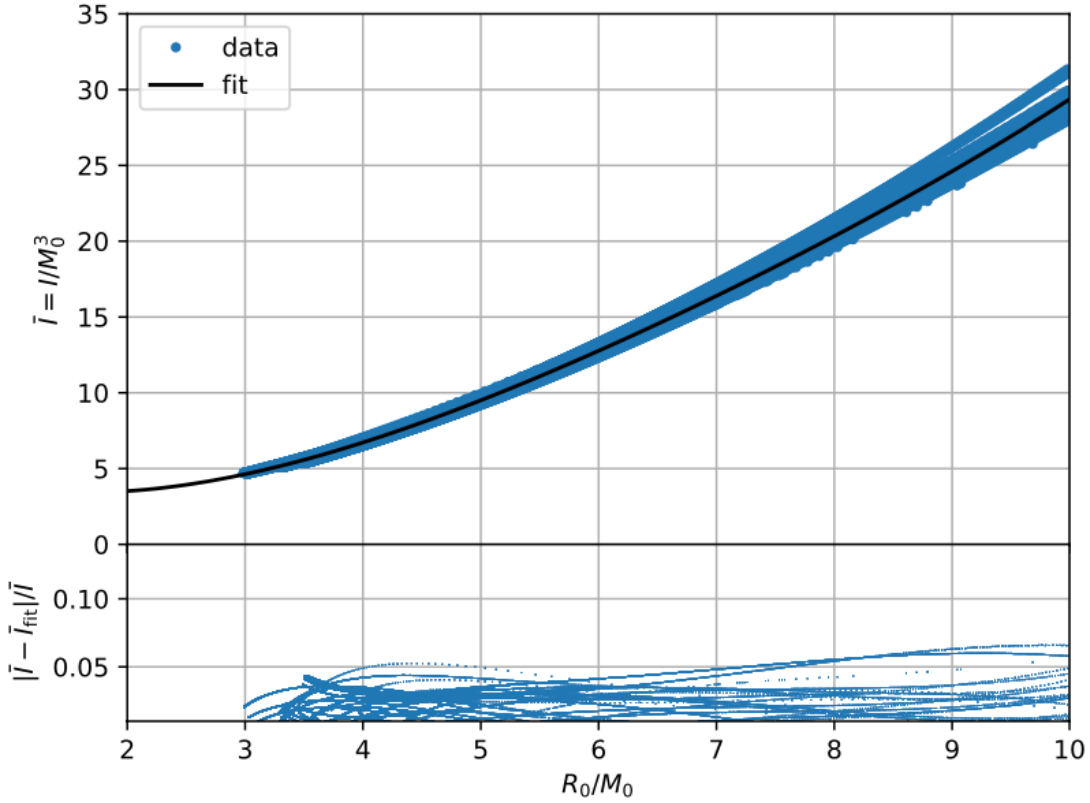

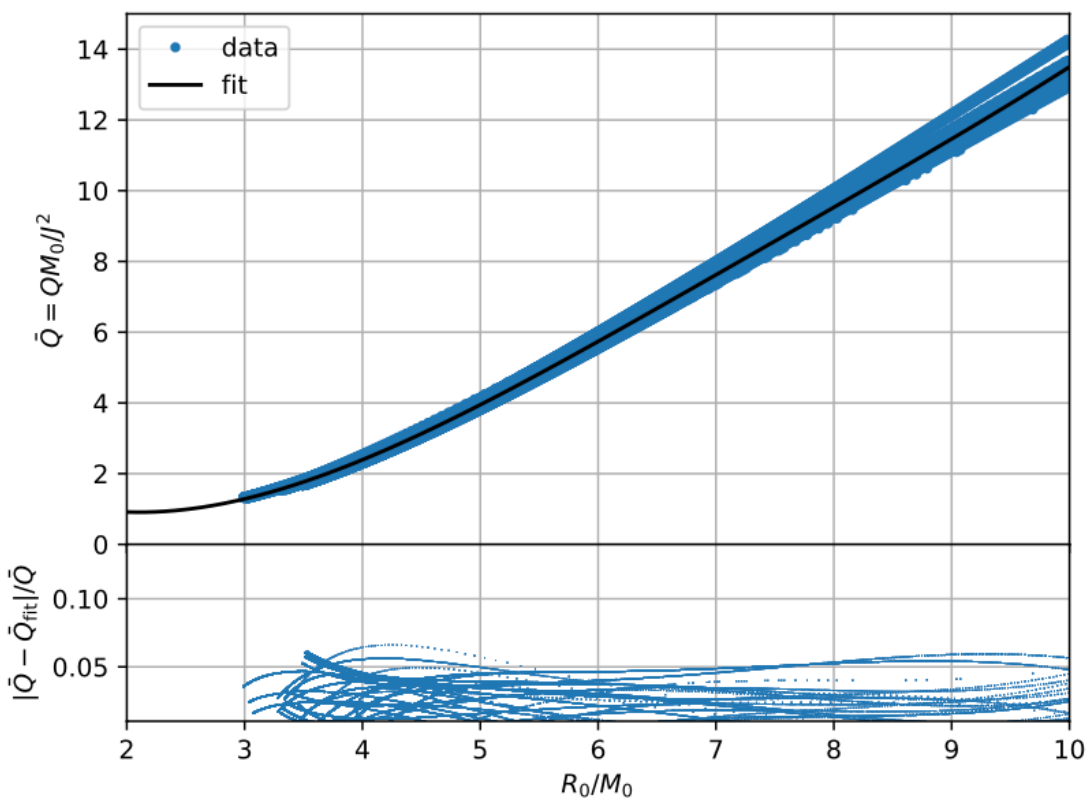

Urbanec +, 2024, in prep

Rotating stars

- Change in shape of the star and total gravitational mass

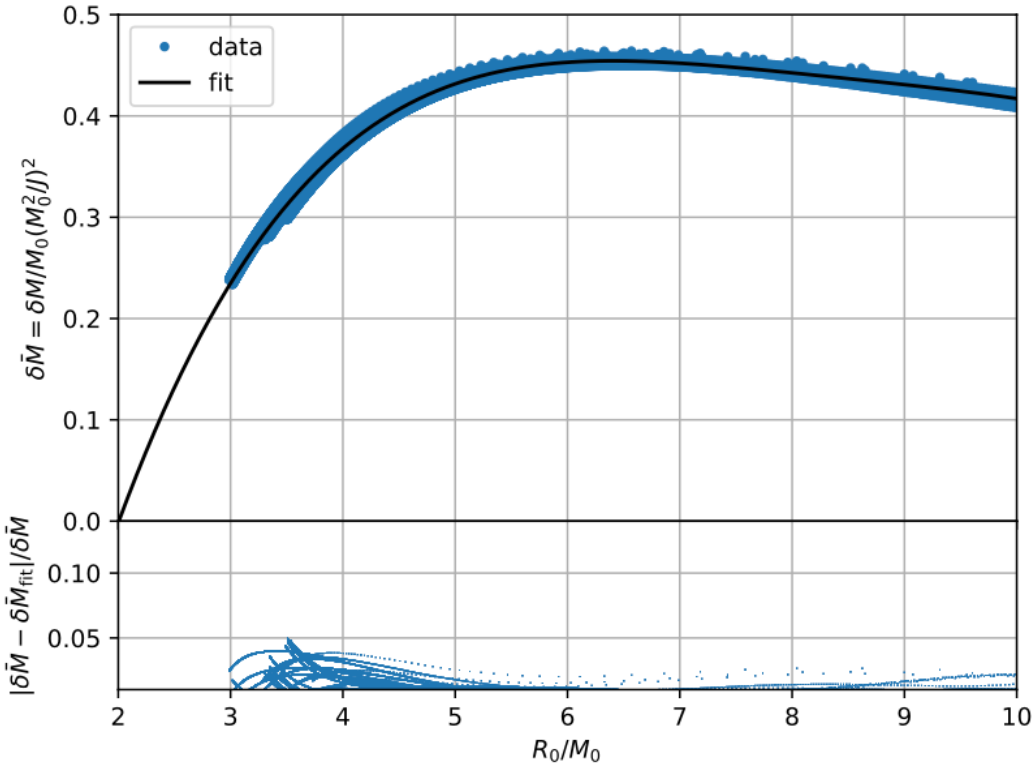

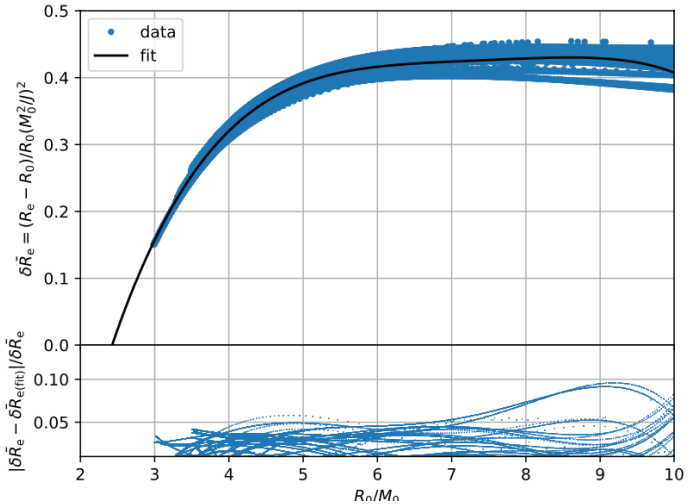

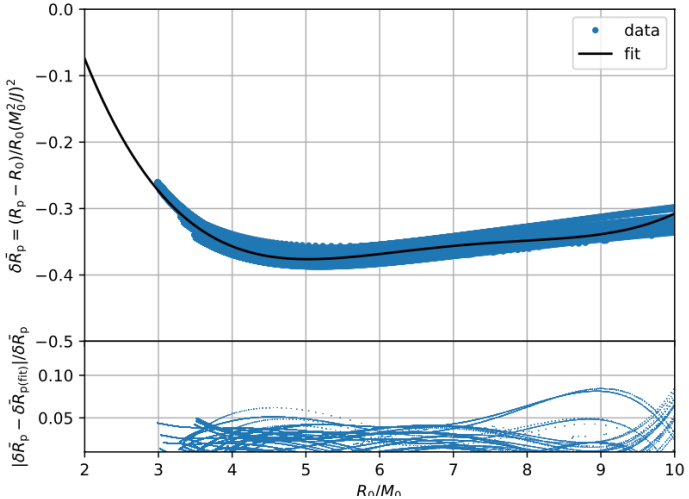

Application of universal relations

- Why using them and why to study them?

- Calculating mass and radius from observations
  - X-ray bursts
  - QPOs
  - GW!

1st detection of GW from binary NS Merger GW170817

- First merger of 2 NS
- Multi-messenger observations
- Measurements of Neutron Star Radii and EoS (1 year later) from tidal deformability
- Other constraints from post-merger evolution

PRL 119, 161101 (2017) Selected for a Viewpoint in *Physics* PHYSICAL REVIEW LETTERS week ending 20 OCTOBER 2017

GW170817: Observation of Gravitational Waves from a Binary Neutron Star Inspiral

B. P. Abbott *et al.**
(LIGO Scientific Collaboration and Virgo Collaboration)
(Received 26 September 2017; revised manuscript received 2 October 2017; published 16 October 2017)

The Astrophysical Journal Letters, 848:L12 (59pp), 2017 October 20 https://doi.org/10.3847/2041-8213/aa91c9
© 2017. The American Astronomical Society. All rights reserved.
OPEN ACCESS

Multi-messenger Observations of a Binary Neutron Star Merger*

LIGO Scientific Collaboration and Virgo Collaboration, Fermi GBM, INTEGRAL, IceCube Collaboration, AstroSat Cadmium Zinc Telluride Imager Team, IPN Collaboration, The Insight-HXMT Collaboration, ANTARES Collaboration, The Swift Collaboration, AGILE Team, The 1M2H Team, The Dark Energy Camera GW-EM Collaboration and the DES Collaboration, The DLT40 Collaboration, GRAWITA: GRAvitational Wave Inaf TeAm, The Fermi Large Area Telescope Collaboration, ATCA: Australia Telescope Compact Array, ASKAP: Australian SKA Pathfinder, Las Cumbres Observatory Group, OzGrav, DWF (Deeper, Wider, Faster Program), AST3, and CAASTRO Collaborations, The VINROUGE Collaboration, MASTER Collaboration, J-GEM, GROWTH, JAGWAR, Caltech-NRAO, TTU-NRAO, and NuSTAR Collaborations, Pan-STARRS, The MAXI Team, TZAC Consortium, KU Collaboration, Nordic Optical Telescope, ePESSTO, GROND, Texas Tech University, SALT Group, TOROS: Transient Robotic Observatory of the South Collaboration, The BOOTES Collaboration, MWA: Murchison Widefield Array, The CALET Collaboration, IKI-GW Follow-up Collaboration, H.E.S.S. Collaboration, LOFAR Collaboration, LWA: Long Wavelength Array, HAWC Collaboration, The Pierre Auger Collaboration, ALMA Collaboration, Euro VLBI Team, Pi of the Sky Collaboration, The Chandra Team at McGill University, DFN: Desert Fireball Network, ATLAS, High Time Resolution Universe Survey, RIMAS and RATIR, and SKA South Africa/MeerKAT
(See the end matter for the full list of authors.)

Received 2017 October 3; revised 2017 October 6; accepted 2017 October 6; published 2017 October 16

Abstract

GW170817: Measurements of Neutron Star Radii and Equation of State

B. P. Abbott *et al.**
(The LIGO Scientific Collaboration and the Virgo Collaboration)

(Received 5 June 2018; revised manuscript received 25 July 2018; published 15 October 2018)

GW170817 Tidal deformabilities

TABLE I. Source properties for GW170817: we give ranges encompassing the 90% credible intervals for different assumptions of the waveform model to bound systematic uncertainty. The mass values are quoted in the frame of the source, accounting for uncertainty in the source redshift.

	Low-spin priors ($\lvert\chi\rvert \leq 0.05$)	High-spin priors ($\lvert\chi\rvert \leq 0.89$)
Primary mass m_1	1.36–1.60 $M_\odot$	1.36–2.26 $M_\odot$
Secondary mass m_2	1.17–1.36 $M_\odot$	0.86–1.36 $M_\odot$
Chirp mass $\mathcal{M}$	$1.188^{+0.004}_{-0.002} M_\odot$	$1.188^{+0.004}_{-0.002} M_\odot$
Mass ratio m_2/m_1	0.7–1.0	0.4–1.0
Total mass $m_{\rm tot}$	$2.74^{+0.04}_{-0.01} M_\odot$	$2.82^{+0.47}_{-0.09} M_\odot$
Radiated energy $E_{\rm rad}$	$> 0.025 M_\odot c^2$	$> 0.025 M_\odot c^2$
Luminosity distance $D_{\rm L}$	40^{+8}_{-14} Mpc	40^{+8}_{-14} Mpc
Viewing angle Θ	$\leq 55°$	$\leq 56°$
Using NGC 4993 location	$\leq 28°$	$\leq 28°$
Combined dimensionless tidal deformability $\tilde{\Lambda}$	≤ 800	≤ 700
Dimensionless tidal deformability $\Lambda(1.4 M_\odot)$	≤ 800	≤ 1400

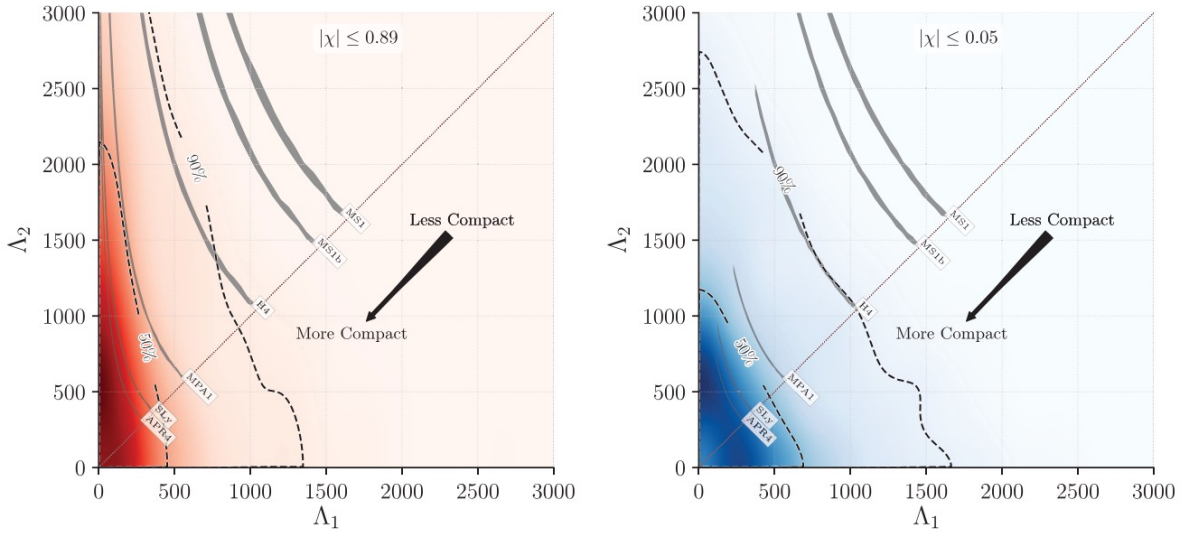

FIG. 5. Probability density for the tidal deformability parameters of the high and low mass components inferred from the detected signals using the post-Newtonian model. Contours enclosing 90% and 50% of the probability density are overlaid (dashed lines). The diagonal dashed line indicates the $\Lambda_1 = \Lambda_2$ boundary. The Λ_1 and Λ_2 parameters characterize the size of the tidally induced mass deformations of each star and are proportional to $k_2(R/m)^5$. Constraints are shown for the high-spin scenario $|\chi| \leq 0.89$ (left panel) and for the low-spin $|\chi| \leq 0.05$ (right panel). As a comparison, we plot predictions for tidal deformability given by a set of representative equations of state [156–160] (shaded filled regions), with labels following [161], all of which support stars of $2.01 M_\odot$. Under the assumption that both components are neutron stars, we apply the function $\Lambda(m)$ prescribed by that equation of state to the 90% most probable region of the component mass posterior distributions shown in Fig. 4. EOS that produce less compact stars, such as MS1 and MS1b, predict Λ values outside our 90% contour.

Selected for a Viewpoint in *Physics*
PRL 119, 161101 (2017) PHYSICAL REVIEW LETTERS week ending 20 OCTOBER 2017

GW170817: Observation of Gravitational Waves from a Binary Neutron Star Inspiral

B. P. Abbott *et al.*[*]
(LIGO Scientific Collaboration and Virgo Collaboration)
(Received 26 September 2017; revised manuscript received 2 October 2017; published 16 October 2017)

GW170817 Mass and Radius Constraints

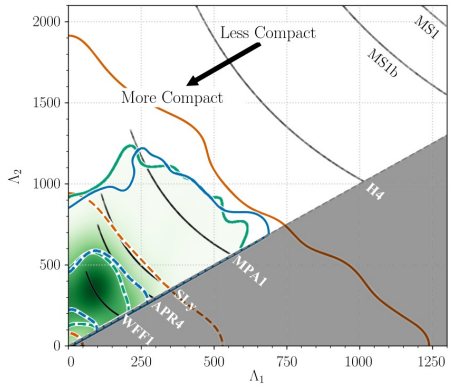

FIG. 1. Marginalized posterior for the tidal deformabilities of the two binary components of GW170817. The green shading shows the posterior obtained using the $\Lambda_a(\Lambda_s, q)$ EOS-insensitive relation to impose a common EOS for the two bodies, while the green, blue, and orange lines denote 50% (dashed) and 90% (solid) credible levels for the posteriors obtained using EOS-insensitive relations, a parametrized EOS without a maximum mass requirement, and independent EOSs (taken from [52]), respectively. The gray shading corresponds to the unphysical region $\Lambda_2 < \Lambda_1$ while the seven black scatter regions give the tidal parameters predicted by characteristic EOS models for this event [113,115,121–125].

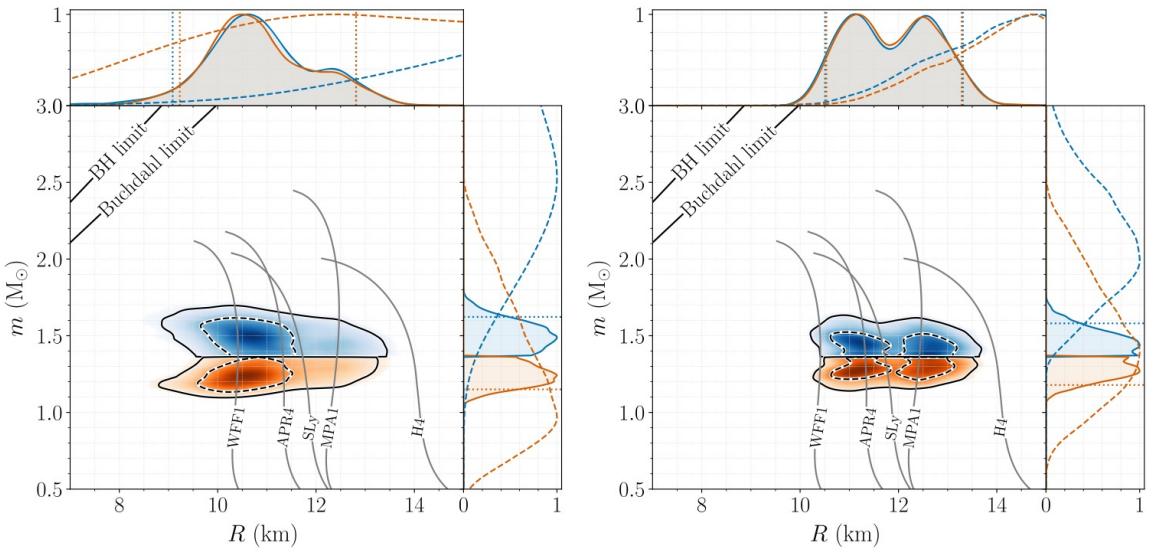

FIG. 3. Marginalized posterior for the mass m and areal radius R of each binary component using EOS-insensitive relations (left panel) and a parametrized EOS where we impose a lower limit on the maximum mass of 1.97 $M_\odot$ (right panel). The top blue (bottom orange) posterior corresponds to the heavier (lighter) NS. Example mass-radius curves for selected EOSs are overplotted in gray. The lines in the top left denote the Schwarzschild BH ($R = 2m$) and Buchdahl ($R = 9m/4$) limits. In the one-dimensional plots, solid lines are used for the posteriors, while dashed lines are used for the corresponding parameter priors. Dotted vertical lines are used for the bounds of the 90% credible intervals.

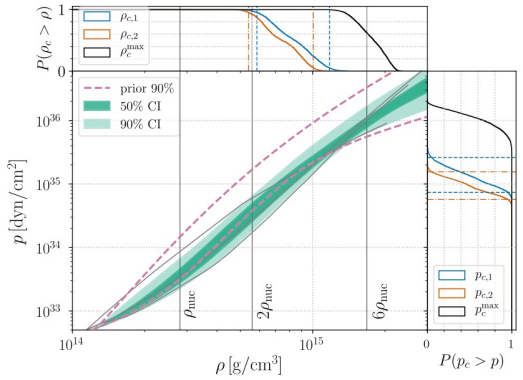

FIG. 2. Marginalized posterior (green bands) and prior (purple dashed) for the pressure p as a function of the rest-mass density ρ of the NS interior using the spectral EOS parametrization and imposing a lower limit on the maximum NS mass supported by the EOS of 1.97 $M_\odot$. The dark (light) shaded region corresponds to the 50% (90%) posterior credible level and the purple dashed lines show the 90% prior credible interval. Vertical lines correspond to once, twice, and six times the nuclear saturation density. Overplotted in gray are representative EOS models [121,122,124], using data taken from [19]; from top to bottom at $2\rho_{nuc}$ we show H4, APR4, and WFF1. The corner plots show cumulative posteriors of central densities ρ_c (top) and central pressures p_c (right) for the two NSs (blue and orange), as well as for the heaviest NS that the EOS supports (black). The 90% credible intervals for ρ_c and p_c are denoted by vertical and horizontal lines respectively for the heavier (blue dashed) and lighter (orange dot-dashed) NS.

GW170817: Measurements of Neutron Star Radii and Equation of State

B. P. Abbott *et al.*[*]

(The LIGO Scientific Collaboration and the Virgo Collaboration)

(Received 5 June 2018; revised manuscript received 25 July 2018; published 15 October 2018)

Conclusions

- Universal relations are great tool that can reduce computational time
- Can be used in various astronomical situations (Xrays, GW etc.)

- There are other universalities not mentioned here
  - Maximum mass at mass shedding limit is given by maximum mass of non-rotating configuration (Breu & Rezzolla 2016 for cold stars; Khosravi Largani + 2022 for hot stars)
  - For all neutron star the specific angular momentum at mass shedding limit is 0.65-0.7 for NS mass $(1.2 – 2.0)M_{\odot}$ (Lo & Lin 2011)

THANK YOU FOR YOUR ATTENTION